Chiral vortical catalysis constrained by LQCD simulations

Ricardo L.S. Farias
Physics Department
Federal University of Santa Maria - Brazil

9th Conference on Chirality, Vorticity and Magnetic Fields in Quantum Matter

São Paulo, July, 2025

Outline

I. Chiral vortical catalysis constrained by LQCD simulations

II. Chiral and Deconfinement Transitions in Spin-Polarized Quark Matter

I. Chiral vortical catalysis constrained by LQCD simulations

- Phd student Rodrigo Nunes - UFSM - Brazil

- William R. Tavares - UERJ - Brazil

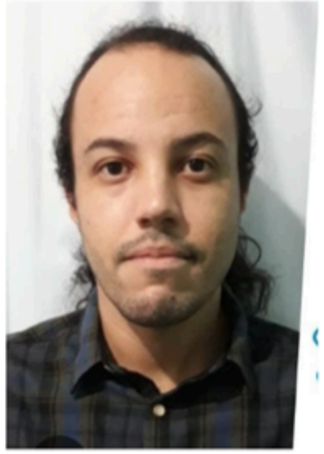

- Varese T. Salvador - UNICAMP - Brazil

R.M. Nunes , **R.L. S. Farias**, W. R. Tavares and V. S.Timóteo , PRD **111**, 056026 (2025)

Motivation

These collisions create most vortical fluid observed to date!!

Non-central HIC

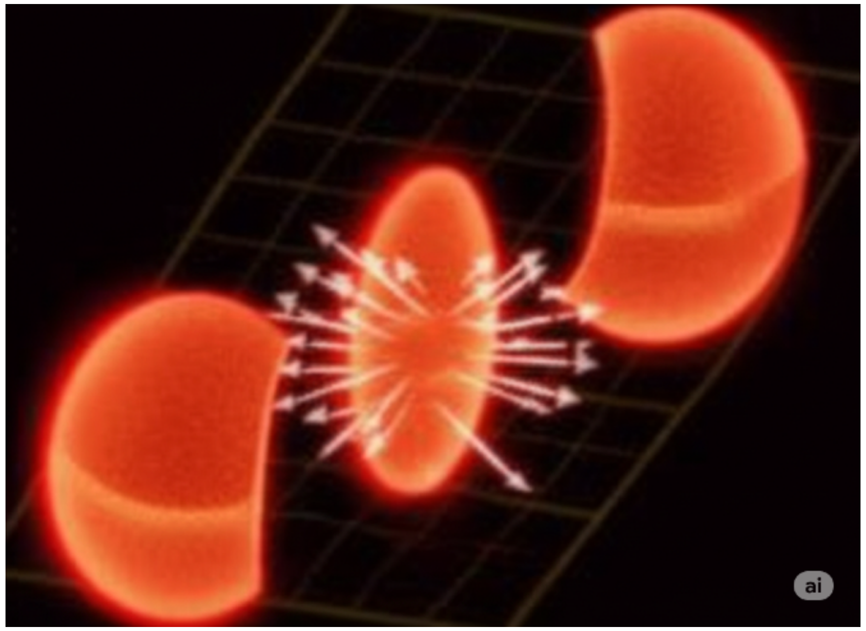

System	Angular Velocity ω [rad/s]
Quark–Gluon Plasma (QGP)	1.52×10^{22} – – 1.52×10^{23}
Pulsars (neutron stars)	4.4×10^{3}
CD / DVD drive	2.0×10^{1} – – 5.0×10^{1}
Ceiling fan (fast mode)	3.0×10^{0} – – 7.0×10^{0}
Tornadoes (core)	$\sim 1.05 \times 10^{1}$
Ferris wheel	1.0×10^{-1} – – 8.0×10^{-1}
Earth	7.29×10^{-5}
Fast bicycle pedaling	$\sim 2.0 \times 10^{1}$
Car engine (max RPM)	$\sim 6.0 \times 10^{2}$ – – 8.4×10^{2}

Table 1: Comparison of Angular Velocities for Various Systems

How does the intrinsic angular momentum of the QGP affect the structure of the QCD phase diagram?

Massive fermions in rotation

To preserve the number of fermions inside the cylindrical cavity it is natural to impose on the fermion wave functions conditions at the boundary of the cylinder

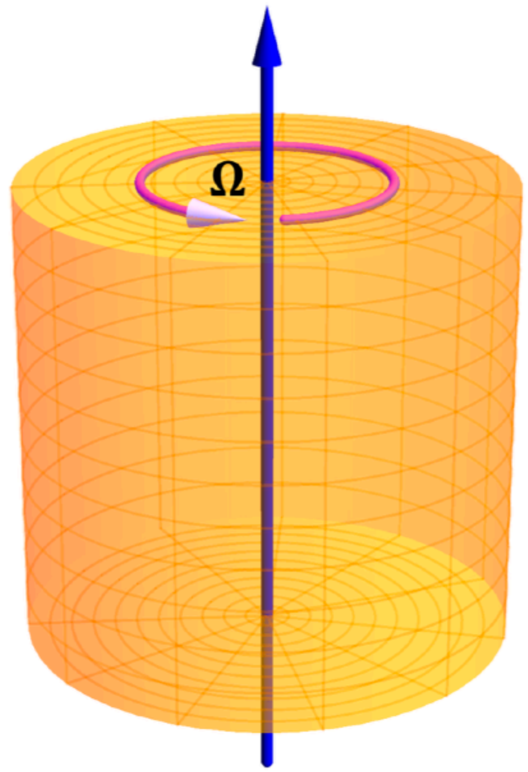

Figure 1. The fermionic medium is uniformly rotating with constant angular velocity Ω inside the cylinder of fixed radius R.

$$g_{\mu\nu} = \begin{pmatrix} 1-(x^2+y^2)\Omega^2 & y\Omega & -x\Omega & 0 \\ y\Omega & -1 & 0 & 0 \\ -x\Omega & 0 & -1 & 0 \\ 0 & 0 & 0 & -1 \end{pmatrix}$$

causality $\rightarrow \Omega\, R < 1$

which corresponds to the line element

$$ds^2 \equiv g_{\mu\nu} dx^\mu dx^\nu = \left(1-\rho^2\Omega^2\right) dt^2 - 2\rho^2\Omega dt d\varphi - d\rho^2 - \rho^2 d\varphi^2 - dz^2$$

M. N. Chernodub and S. Gongyo, JHEP 01 (2017) 136

Motivation

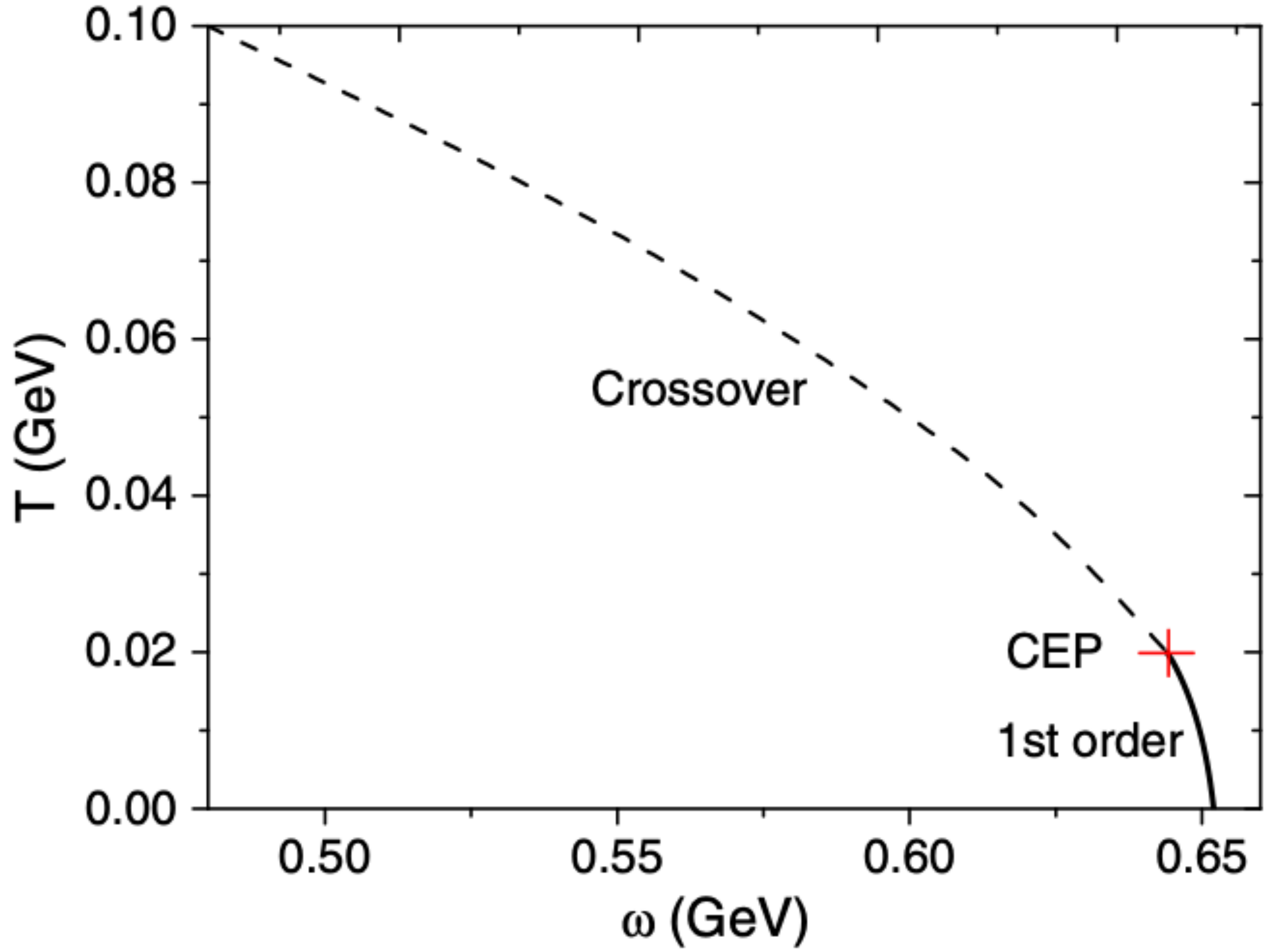

SU(2) NJL model

PRL **117,** 192302 (2016) PHYSICAL REVIEW LETTERS

Pairing Phase Transitions of Matter under Rotation

Yin Jiang[1,*] and Jinfeng Liao[1,2,†]

Motivation

Hao-Lei Chen, Xu-Guang Huang, and Jinfeng Liao

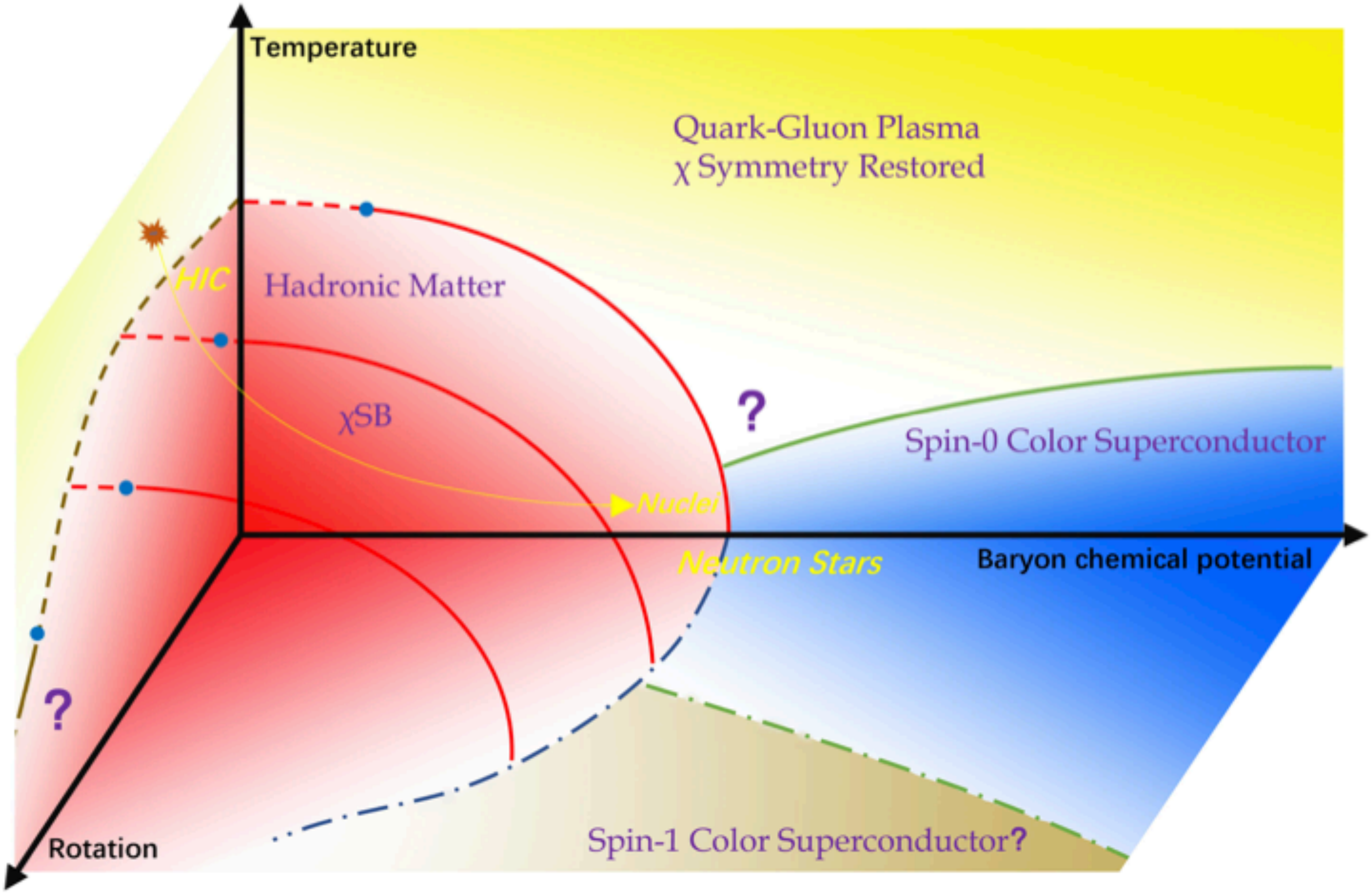

Lattice QCD Results (v_I)

Imaginary v_I

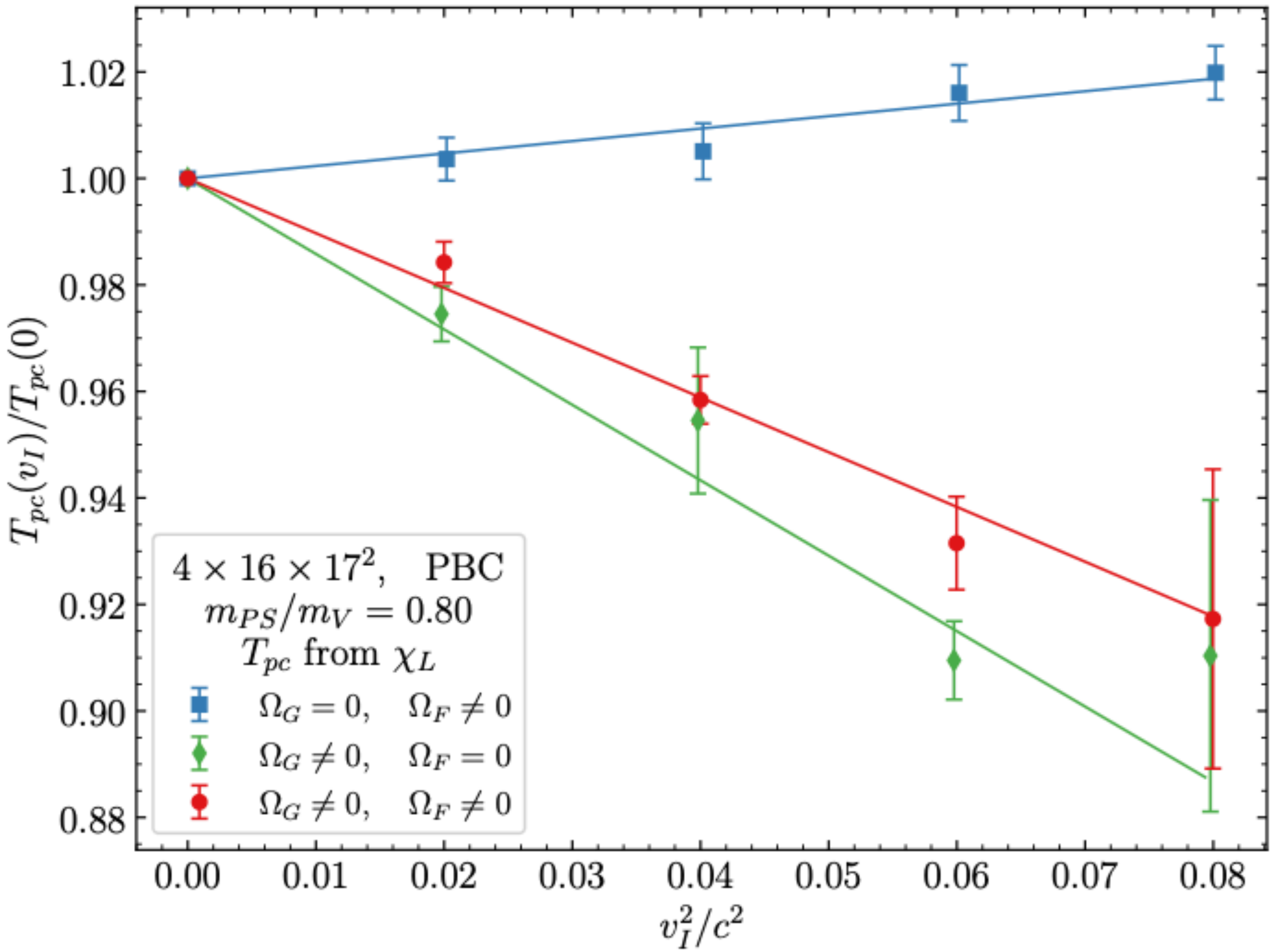

V.V. Braguta, A. Kotov and A. Roenko, PoS LATTICE2022 (2023) 190

Lattice QCD Results

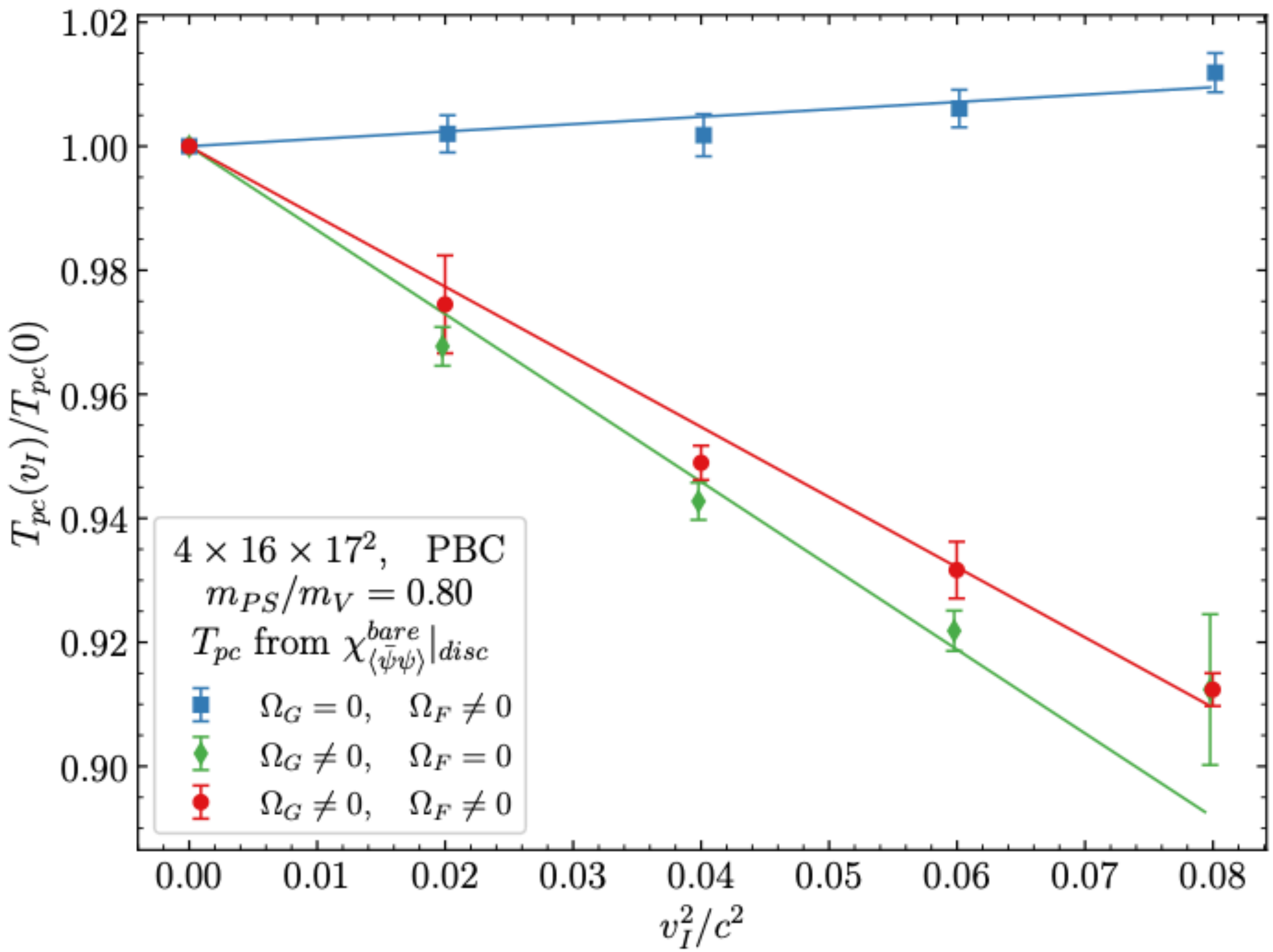

$$\frac{T_{pc}(v_I)}{T_{pc}(0)} = 1 - B_2 v_I^2$$

$$\frac{T_{pc}(v)}{T_{pc}(0)} = 1 + B_2 v^2$$

V.V. Braguta, A. Kotov and A. Roenko, PoS LATTICE2022 (2023) 190

This presents a puzzle regarding the QCD phase transition under rotation

- The resolution of this puzzle is still an open question
- A rigorous QCD calculation is still necessary
- Additional lattice data are welcome

SU(2) NJL model

$$\mathcal{L}_{NJL} = \bar{\psi}\left(\not{D} - m\right)\psi + G\left[(\bar{\psi}\psi)^2 + (\bar{\psi}i\gamma_5\vec{\tau}\psi)^2\right]$$

good **chiral** physics, pions,…
BUT no confinement

G, Λ and m_c → m_π, f_π and $\langle\bar{\psi}\psi\rangle$

$$\mathcal{F} = \frac{(M - m_c)^2}{4G} - N_c \sum_{f,s} \int \frac{d^4p}{(2\pi)^4} \ln\left[p^2 + M^2\right]$$

And the gap equation: $\partial\mathcal{F}/\partial M = 0 \longrightarrow \infty$

Y. Nambu and G. Jona-Lasinio, Phys. Rev. **122**, 345 (1961)

Motivation

Lattice QCD Results -> gluon effects are very important!

How to mimic the gluon effects?

$$G \to G(\omega)$$

We use lattice data for $T_c X \omega$ as input!

$G(\omega)$

Numerical Results

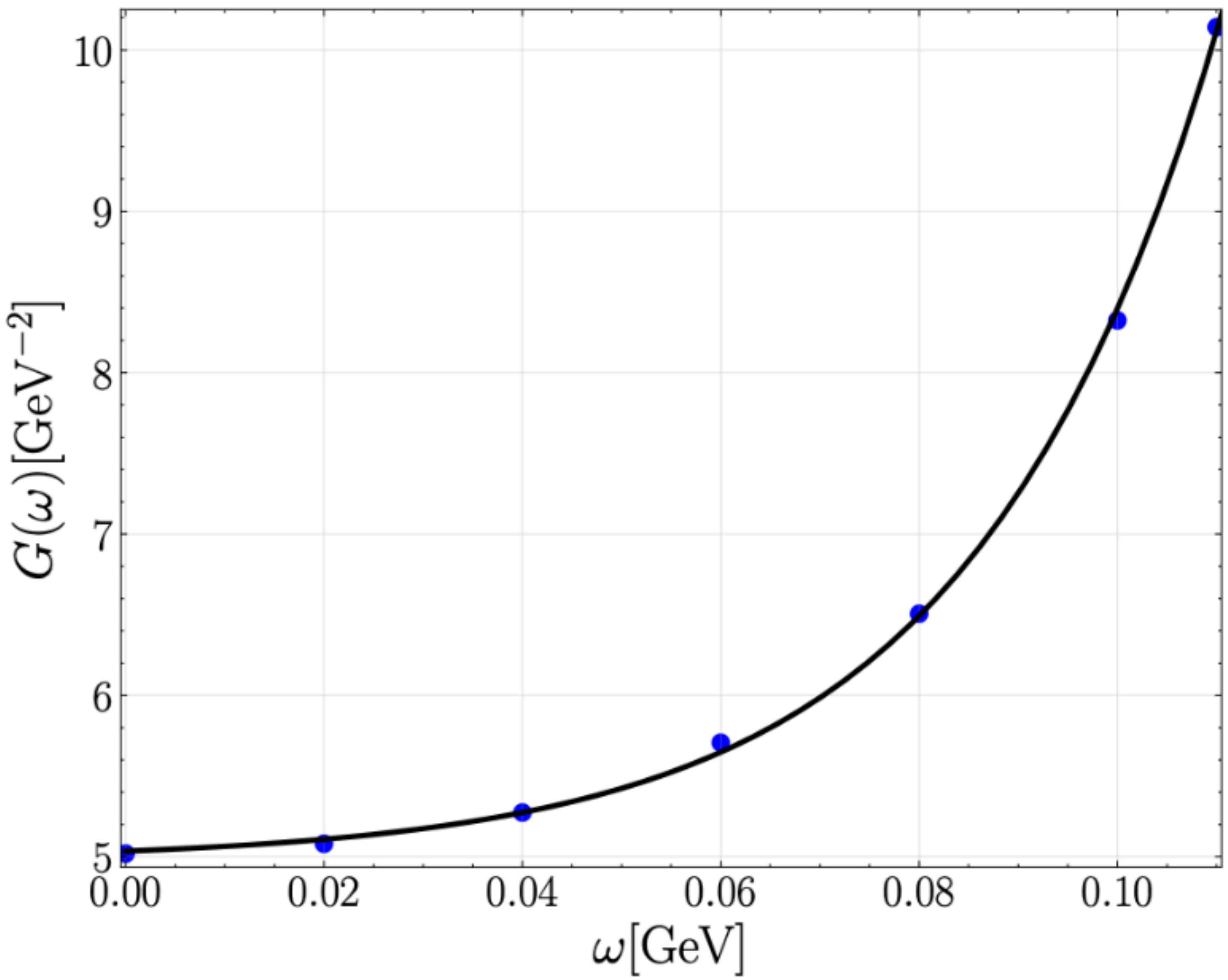

$$G(\omega) = G_\alpha + G_\beta \ \exp\left(\frac{\omega}{G_\gamma}\right)$$

where $G_\alpha = 4.97667 \ \mathrm{GeV}^{-2}$, $G_\beta = 0.05840 \ \mathrm{GeV}^{-2}$ and $G_\gamma = 0.02457 \ \mathrm{GeV}$.
$r = 5 \ \mathrm{GeV}^{-1}$, $\Lambda = 651 \ \mathrm{MeV}$ and $m = 5.5 \ \mathrm{MeV}$

R.M. Nunes , **R.L. S. Farias**, W. R. Tavares and V. S.Timóteo , PRD **111**, 056026 (2025)

Numerical Results

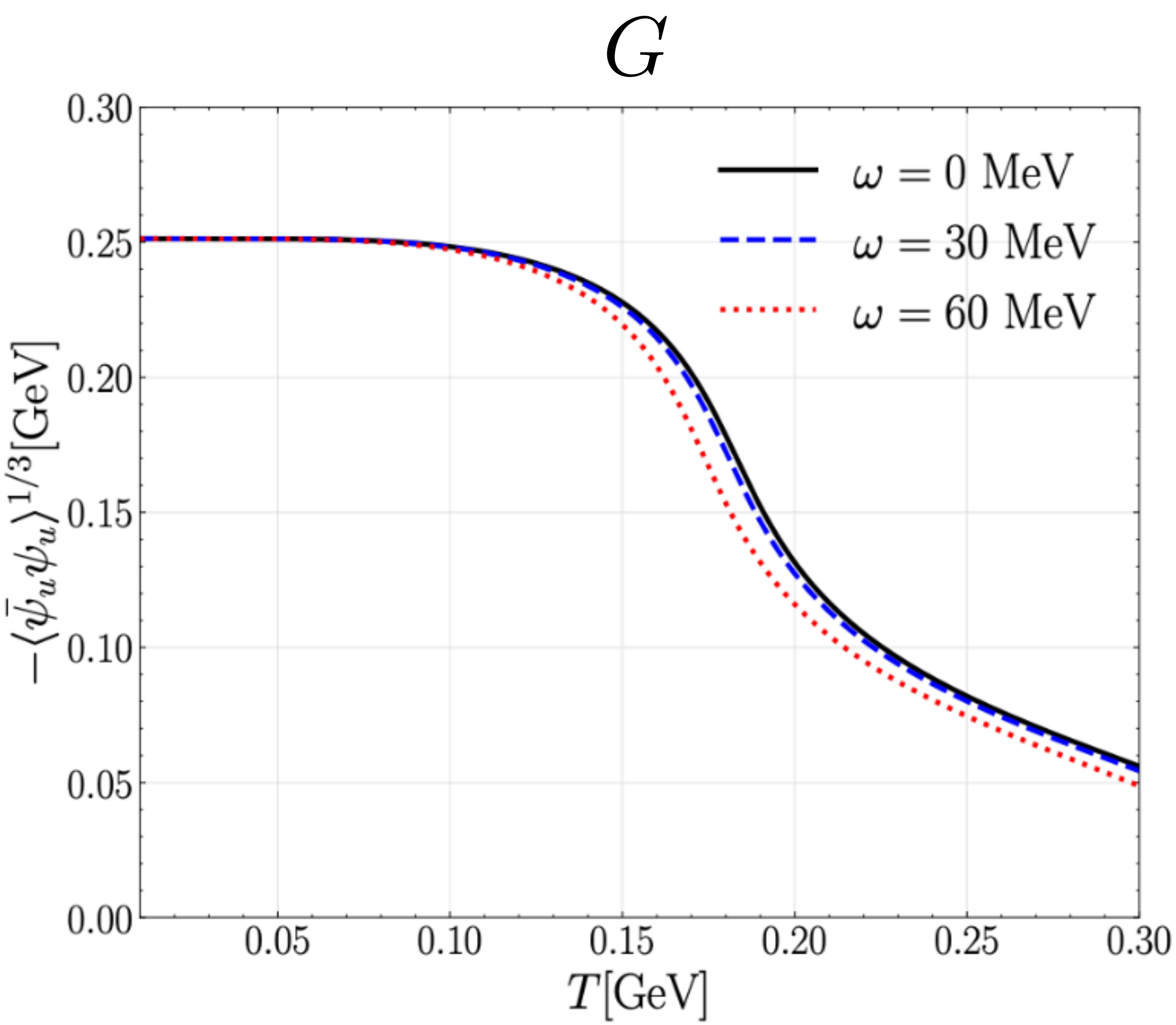

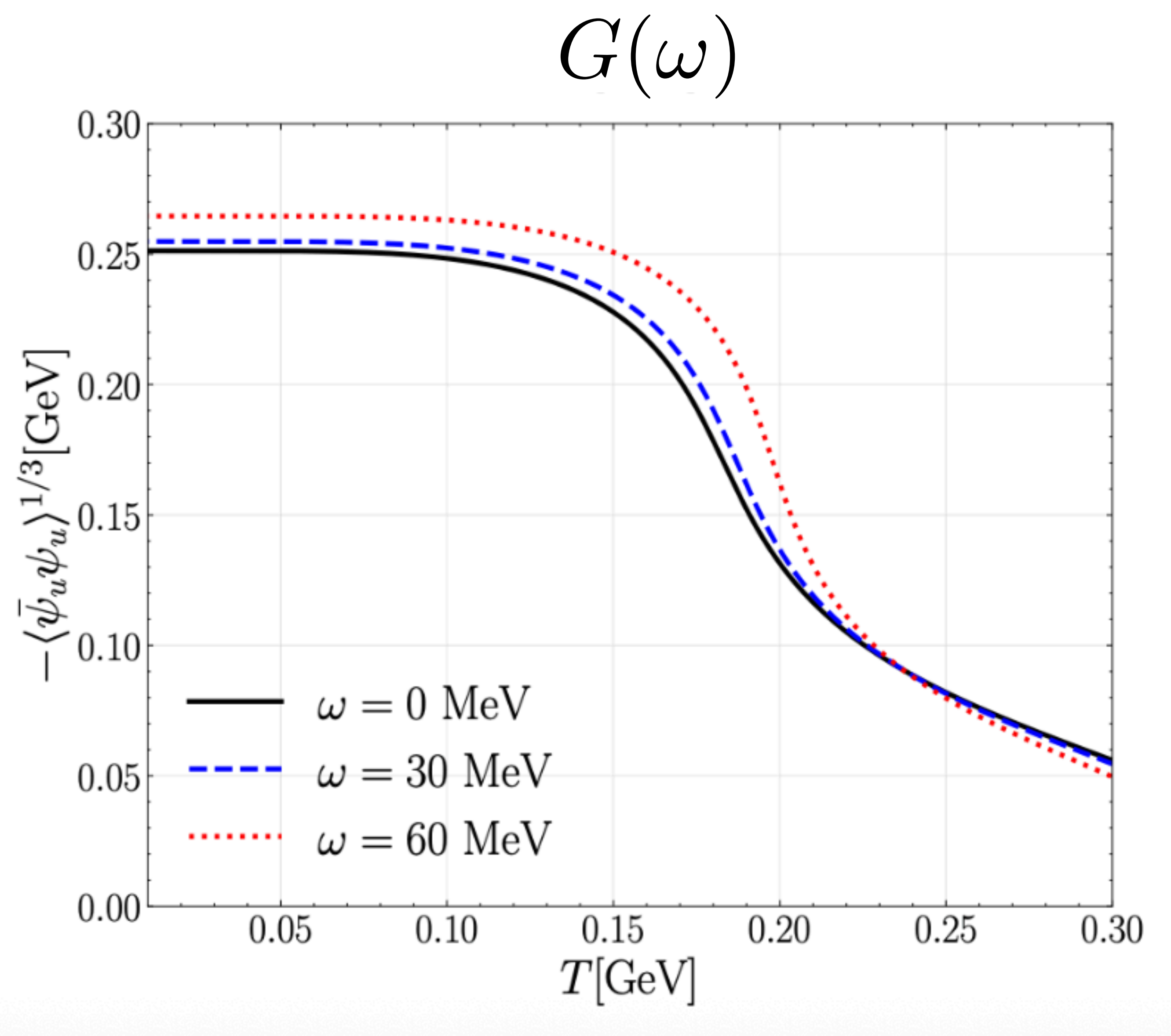

R.M. Nunes , **R.L. S. Farias**, W. R. Tavares and V. S.Timóteo , PRD **111**, 056026 (2025)

Numerical Results

G

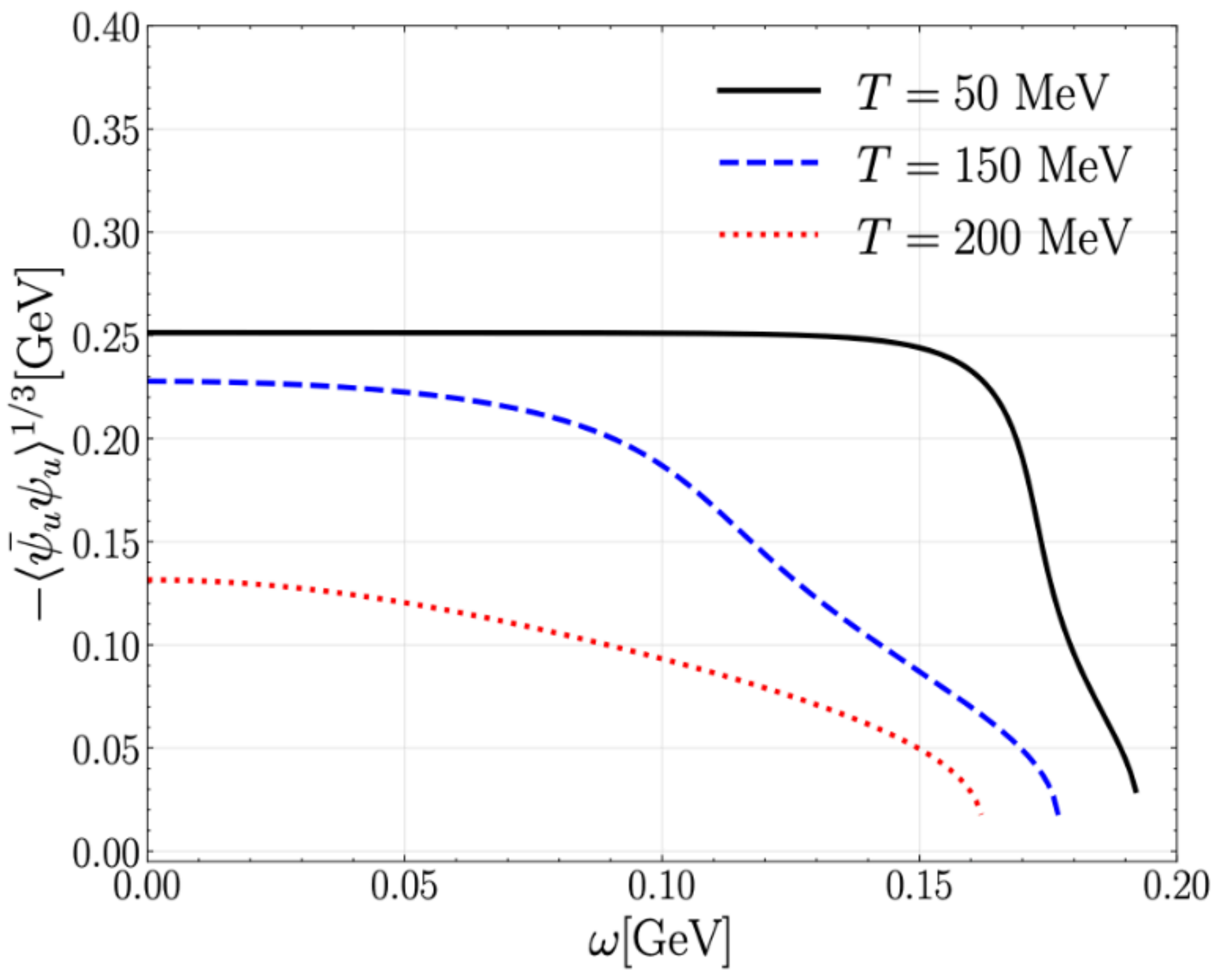

$G(\omega)$

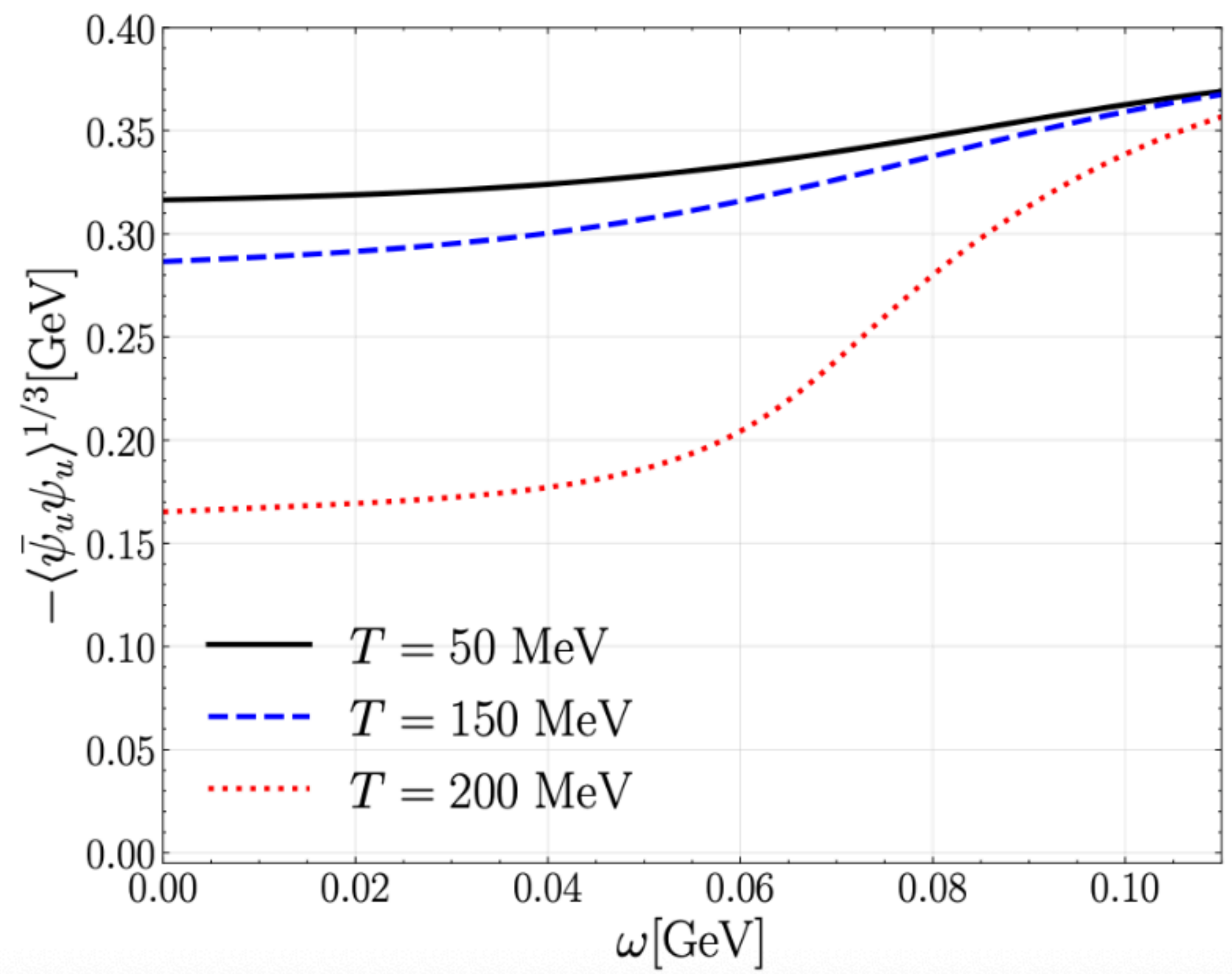

R.M. Nunes , **R.L. S. Farias**, W. R. Tavares and V. S.Timóteo , PRD **111**, 056026 (2025)

Numerical Results

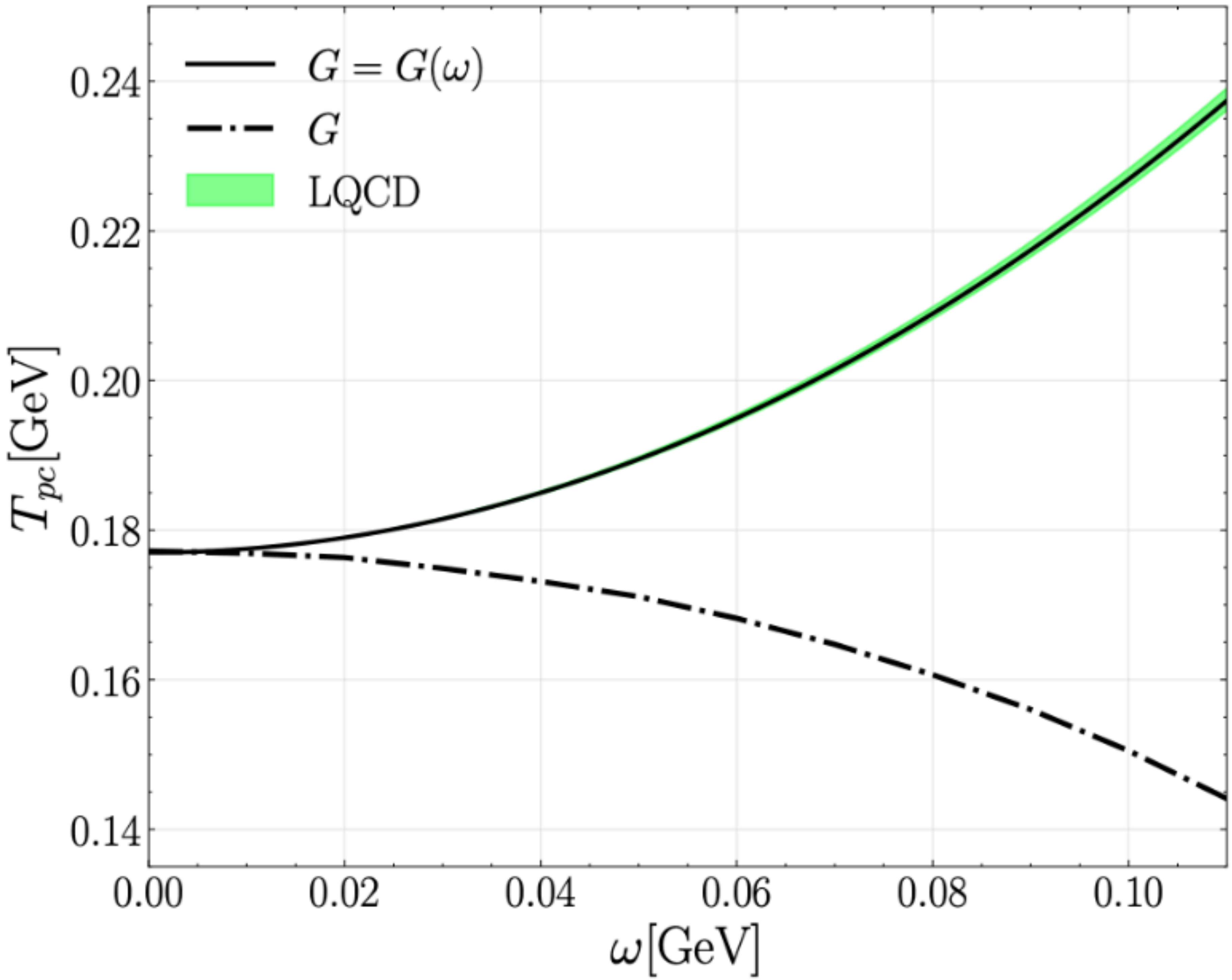

R.M. Nunes , **R.L. S. Farias**, W. R. Tavares and V. S.Timóteo , PRD **111**, 056026 (2025)

Extrapolation to QCD Phase Diagram

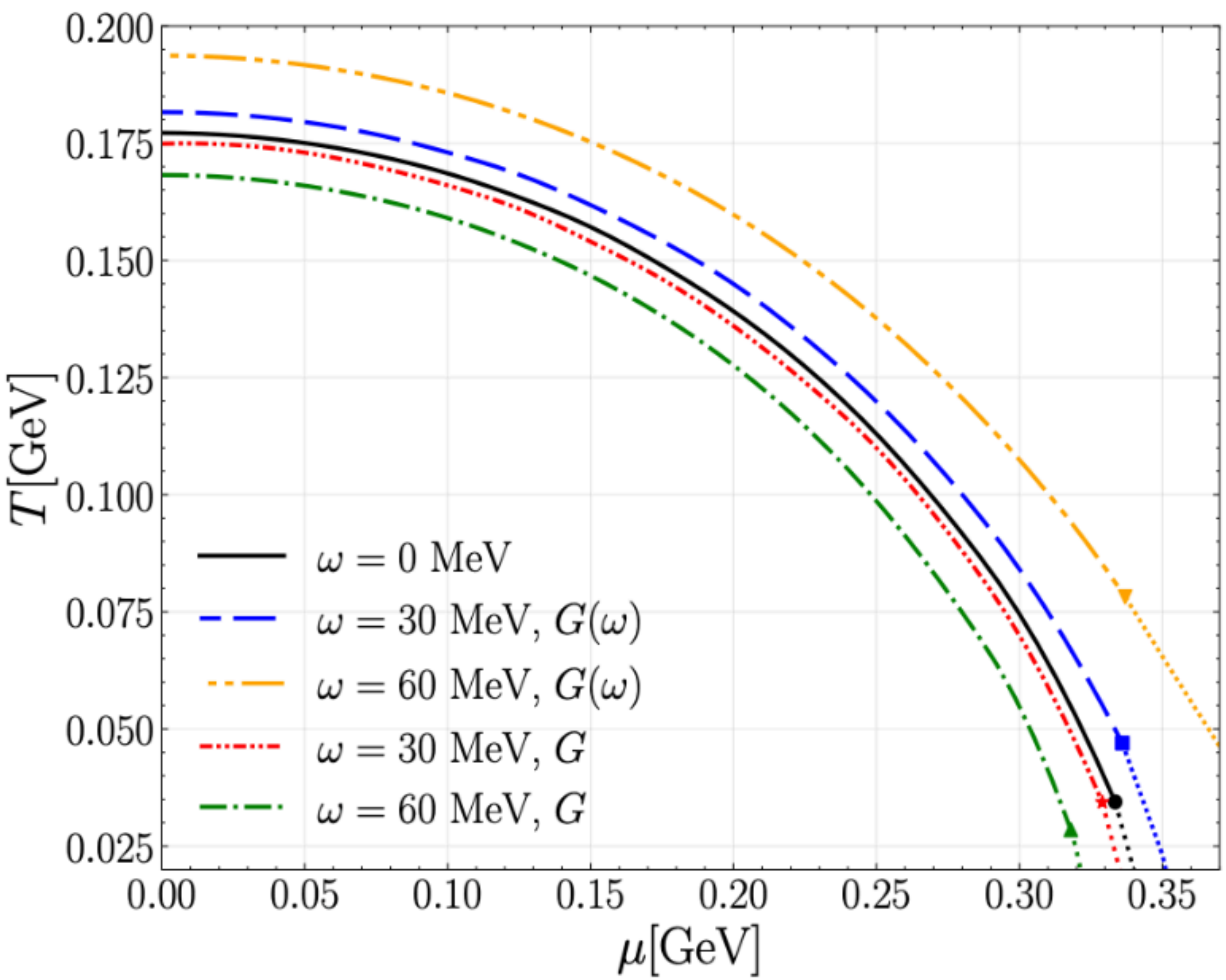

R.M. Nunes , **R.L. S. Farias**, W. R. Tavares and V. S.Timóteo , PRD **111**, 056026 (2025)

Extrapolation to QCD Phase Diagram

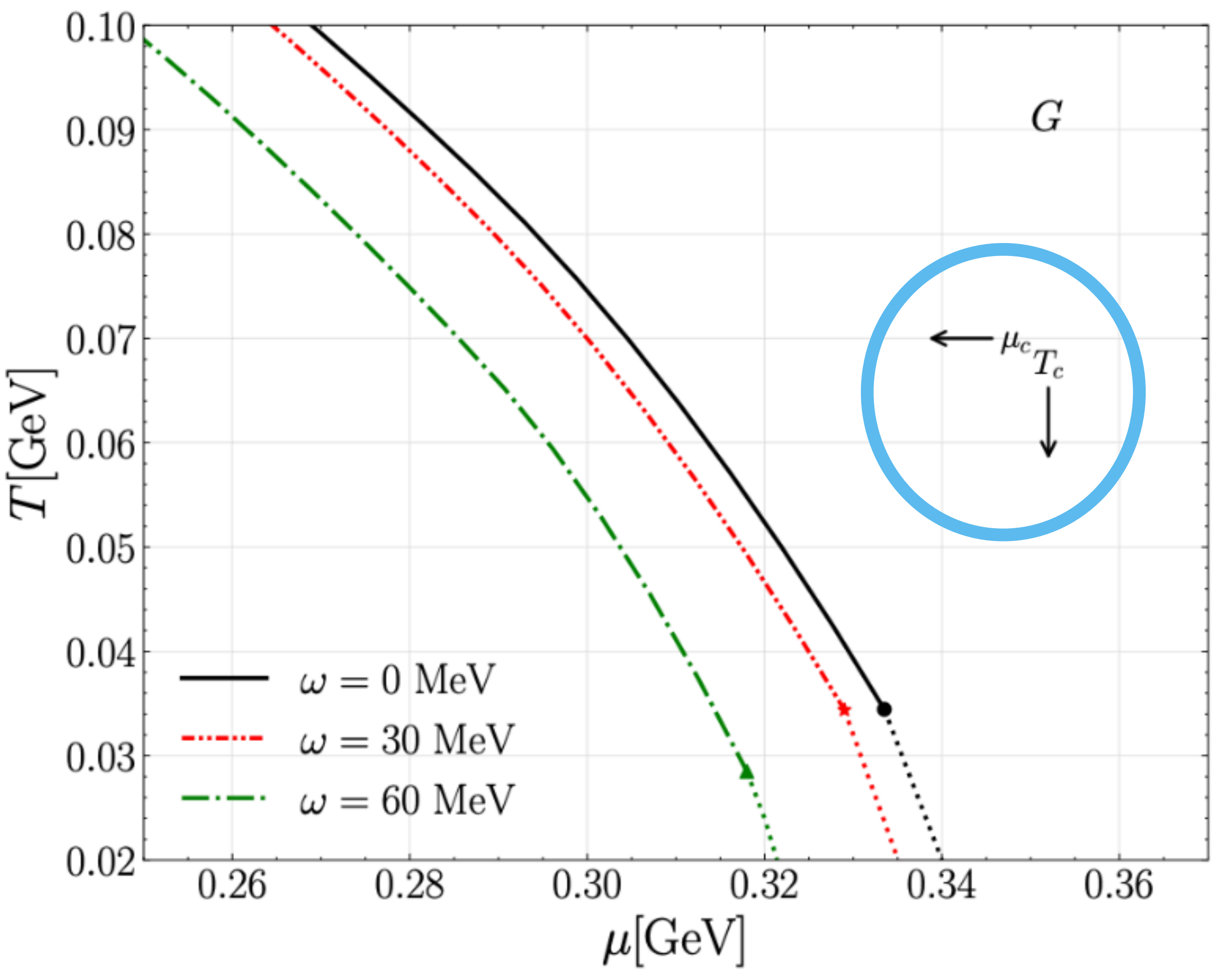

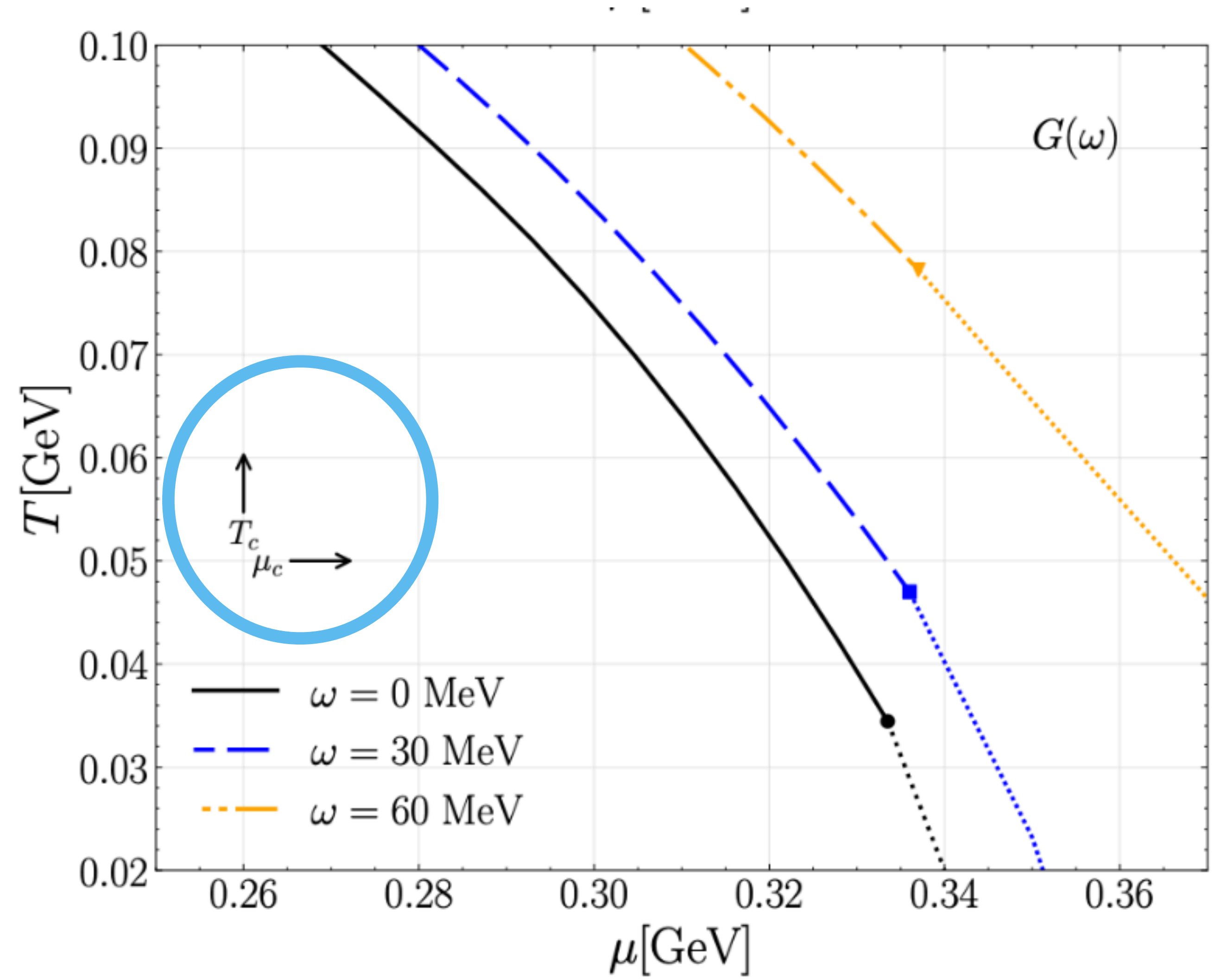

R.M. Nunes , **R.L. S. Farias**, W. R. Tavares and V. S.Timóteo , PRD **111**, 056026 (2025)

Conclusion

The running coupling enhances the chiral condensate as a function of angular velocity, thereby strengthening chiral symmetry breaking —

an effect known as

chiral vortical catalysis

Y. Jiang, Eur. Phys. J. C 82, 949 (2022)
R.M. Nunes , **R.L. S. Farias**, W. R. Tavares and V. S.Timóteo , PRD **111**, 056026 (2025)

II - Chiral and Deconfinement Transitions in **Spin-Polarized** Quark Matter

In Collaboration with:

- William R. Tavares - UERJ - Brazil

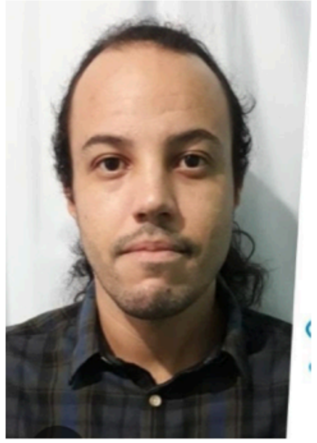

Chiral and Deconfinement Transitions in Spin-Polarized Quark Matter

R. L. S. Farias[1] and William R. Tavares[2]

[1] *Departamento de Física, Universidade Federal de Santa Maria, 97105-900, Santa Maria, RS, Brazil*
[2] *Departamento de Física Teórica, Universidade do Estado do Rio de Janeiro, 20550-013 Rio de Janeiro, RJ, Brazil*

We investigate the influence of spin polarization in strongly interacting matter by introducing a finite spin potential, μ_Σ, which effectively controls the spin density of the system without requiring rotation or specific boundary conditions. Inspired by recent lattice QCD simulations that incorporated such a potential, we implement this approach within an effective QCD framework. Our results show that increasing spin polarization leads to a simultaneous decrease in both the chiral and deconfinement restoration temperatures. The resulting phase structure is qualitatively consistent with lattice findings, and notably, we observe the emergence of a first-order chiral phase transition at zero temperature. These results suggest that spin-polarized environments can significantly impact the QCD phase diagram and offer a controlled route for studying spin effects in hot and dense matter.

Motivation

In high-energy physics, numerous key measurements are closely connected to the concept of spin:

- proton spin crisis
- single spin asymmetry and transverse polarization of hyperons
- muon anomalous magnetic dipole moment
- the neutron electric dipole moment

In HIC, numerous key measurements are closely connected to the concept of spin:

- chiral magnetic effect
- spin polarization
- chiral separation effect
- …

Chiral and Deconfinement Transitions in Spin-Polarized Quark Matter

PHYSICAL REVIEW D **111,** 114508 (2025)

Chiral and deconfinement thermal transitions at finite quark spin polarization in lattice QCD simulations

V. V. Braguta,[1,*] M. N. Chernodub,[2,3,†] and A. A. Roenko[1,‡]

[1]*Bogoliubov Laboratory of Theoretical Physics, Joint Institute for Nuclear Research, Dubna 141980 Russia*

[2]*Institut Denis Poisson, CNRS-UMR 7013, Université de Tours, 37200 France*

[3]*Department of Physics, West University of Timişoara, Boulevard Vasile Pârvan 4, Timişoara 300223, Romania*

Quark spin potential

The quark spin density can be introduced via a modification to the Dirac Lagrangian:

$$\delta_\Sigma \mathcal{L}_q = \mu_{\alpha,\mu\nu} \overline{\psi} \mathcal{S}^{\alpha,\mu\nu} \psi \,,$$

where the relativistic spin density matrix is defined by

$$\mathcal{S}^{\alpha,\mu\nu} = \frac{1}{2} \{\gamma^\alpha, \Sigma^{\mu\nu}\} \,, \qquad \Sigma^{\mu\nu} = \frac{i}{4} [\gamma^\mu, \gamma^\nu] \,.$$

Assuming spin polarization along the z axis, we choose the background spin field as

$$\mu_{\alpha,\mu\nu} = \frac{\mu_\Sigma}{2} \delta_{\alpha 0} \left(\delta_{\mu 1}\delta_{\nu 2} - \delta_{\nu 1}\delta_{\mu 2}\right) ,$$

which leads to a simplified Lagrangian:

$$\delta_\Sigma \mathcal{L}_q = \mu_\Sigma \overline{\psi} \gamma^0 \Sigma^{12} \psi.$$

In the Dirac basis, the spin term becomes

$$\gamma^0 \Sigma^{12} = \frac{1}{2} \gamma^3 \gamma^5 = \mathrm{diag}\left(+\tfrac{1}{2}, -\tfrac{1}{2}, -\tfrac{1}{2}, +\tfrac{1}{2}\right) .$$

V. V. Braguta, M. N. Chernodub and A. A. Roenko, PRD **111**, 114508 (2025)

Quark spin potential

The spin potential μ_Σ plays a role similar to a chemical potential, determining the energy cost to add a spin-$\frac{1}{2}$ particle with spin up or down:

$$\delta E_\uparrow = +\frac{\mu_\Sigma}{2}, \qquad \delta E_\downarrow = -\frac{\mu_\Sigma}{2}.$$

Therefore, $\mu_\Sigma = \delta E_\uparrow - \delta E_\downarrow$ quantifies the spin imbalance in the system and serves as a thermodynamic parameter.

This spin potential is structurally analogous to the angular velocity Ω of a rotating frame. In such a frame, the quark Lagrangian acquires an additional term:

$$\delta_\Omega \mathcal{L}_q = \Omega\, \overline{\psi} \left[i(-x\partial_y + y\partial_x) + \gamma^0 \Sigma^{12} \right] \psi,$$

where the first term represents the orbital angular momentum and the second, the spin-rotation coupling. If one sets $\Omega = \mu_\Sigma$, the spin-polarization term in rotation coincides with the static medium term, indicating a close analogy between spin potential and rotational effects.

V. V. Braguta, M. N. Chernodub and A. A. Roenko, PRD **111**, 114508 (2025)

Dirac Equation at finite spin potential

$$(i\gamma^\mu \partial_\mu - M + \frac{\mu_\Sigma}{2}\gamma_3\gamma_5)\psi = 0$$

Dispersion Relation

$$E_s = \sqrt{p_\perp^2 + \left(\sqrt{p_3^2 + M^2} + s\frac{\mu_\Sigma}{2}\right)^2}$$

where $p_\perp^2 = p_1^2 + p_2^2$

EPNJL model

$$\mathcal{L} = \overline{\psi}\left(iD_\mu\gamma^\mu - m_c + \frac{\mu_\Sigma}{2}\gamma^3\gamma^5\right)\psi + G\left[(\overline{\psi}\psi)^2 + (\overline{\psi}i\gamma_5\vec{\tau}\psi)^2\right] - \mathcal{U}(l,\bar{l},T)$$

$$\frac{\mathcal{U}(l,\bar{l},T)}{T^4} = -\frac{a(T)l\bar{l}}{2} + b(T)\log\left[1 - 6l\bar{l} + 4(l^3+\bar{l}^3) - 3(l\bar{l})^2\right]$$

where $a(T)$ and $b(T)$ is given by

$$a(T) = a_0 + a_1\left(\frac{T_0}{T}\right) + a_2\left(\frac{T_0}{T}\right)^2$$

$$b(T) = b_3\left(\frac{T_0}{T}\right)^3$$

The inclusion of the entanglement is given by the change on the coupling

$$G \to G(l,\bar{l}) = G\left[1 - \alpha_1 l\bar{l} - \alpha_2(l^3+\bar{l}^3)\right]$$

where $\alpha_1 = \alpha_2 = 0.2$.

EPNJL model

$$V(M,l,l^\dagger,T,\mu) = \mathcal{U}\left(l,l^\dagger,T\right) + \frac{(M-m_0)^2}{4G(l,\bar{l})} + V_{Vac} - \frac{N_f}{\beta}\sum_{s=\pm1}\int\frac{d^3p}{(2\pi)^3}\left[\log\left(F_+^s F_-^s\right)\right]$$

where $\beta = T^{-1}$, $E_s^2(p_3,p_\perp) = p_\perp^2 + \left(\sqrt{p_3^2+M^2} + s\frac{\mu_\Sigma}{2}\right)^2$ and we have adopted the following definitions

$$V_{Vac} = -N_c N_f \sum_{s=\pm1}\int\frac{dp_3 dp_\perp\ p_\perp}{2\pi^2}E_s(p_3,p_\perp)$$

$$F_-^s = 1 + 3le^{-\beta(E_s-\mu)} + 3l^\dagger e^{-2\beta(E_s-\mu)} + e^{-3\beta(E_s-\mu)}$$

$$F_+^s = 1 + 3l^\dagger e^{-\beta(E_s+\mu)} + 3le^{-2\beta(E_s+\mu)} + e^{-3\beta(E_s+\mu)}$$

Minimizing thermodynamic potential, $V(M,l,l^\dagger,T,\mu)$ with respect to M, l, and $l^\dagger$, we obtain the three Gap equations :

$$\frac{\partial V(M,l,l^\dagger,T,\mu)}{\partial M} = \frac{\partial V(M,l,l^\dagger,T,\mu)}{\partial l} = \frac{\partial V(M,l,l^\dagger,T,\mu)}{\partial l^\dagger} = 0$$

Numerical Results

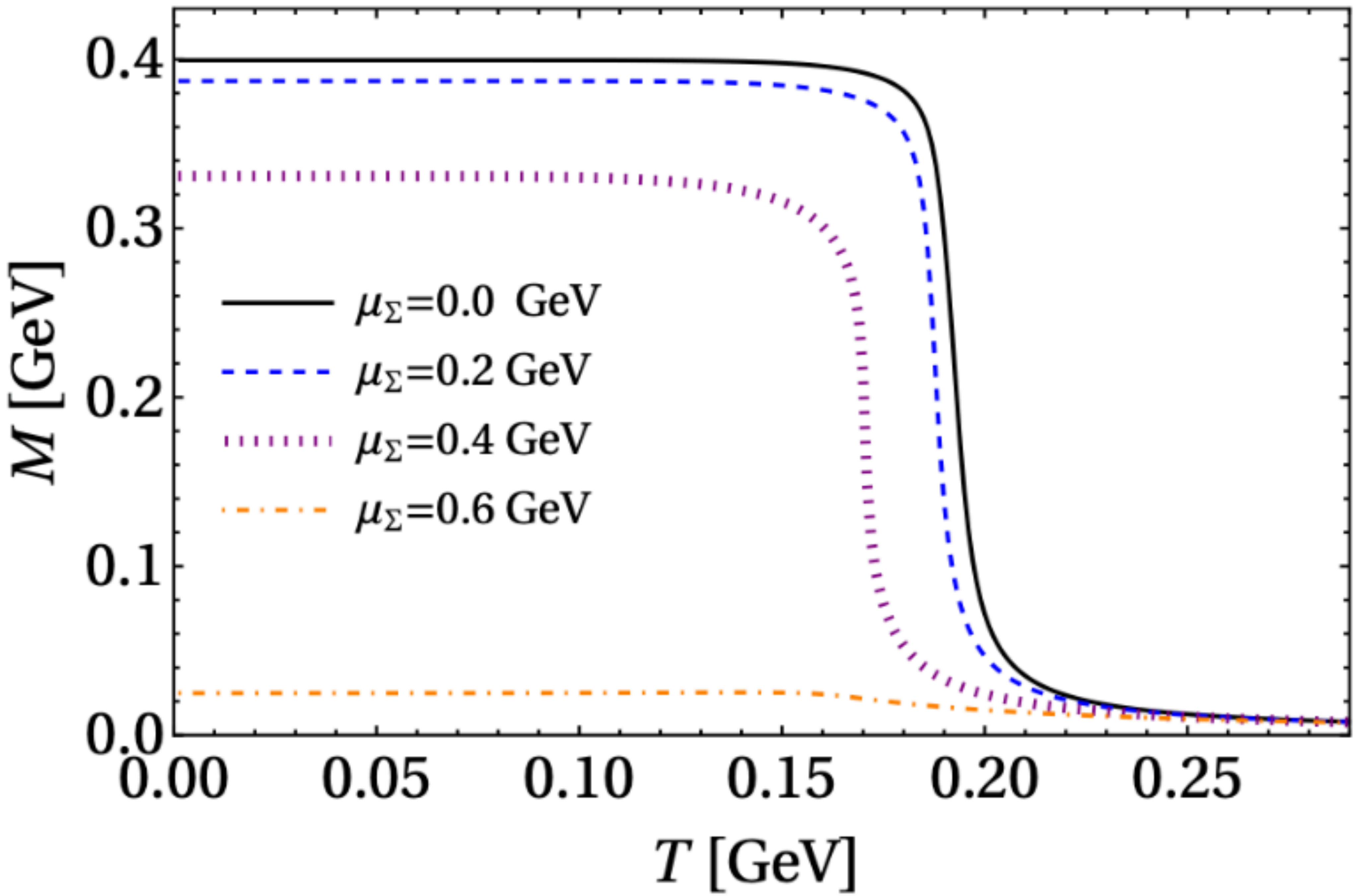

Numerical Results

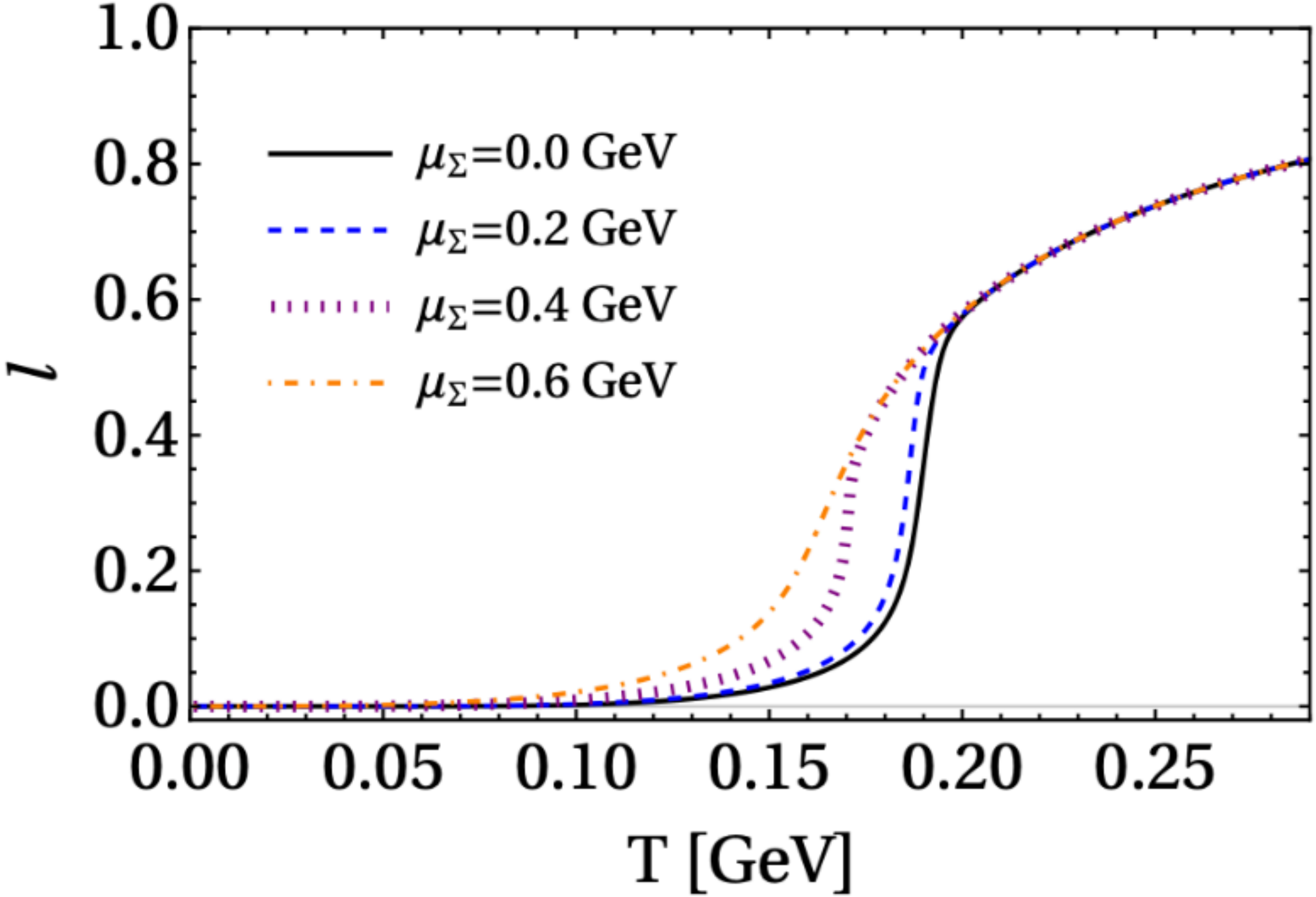

Numerical Results

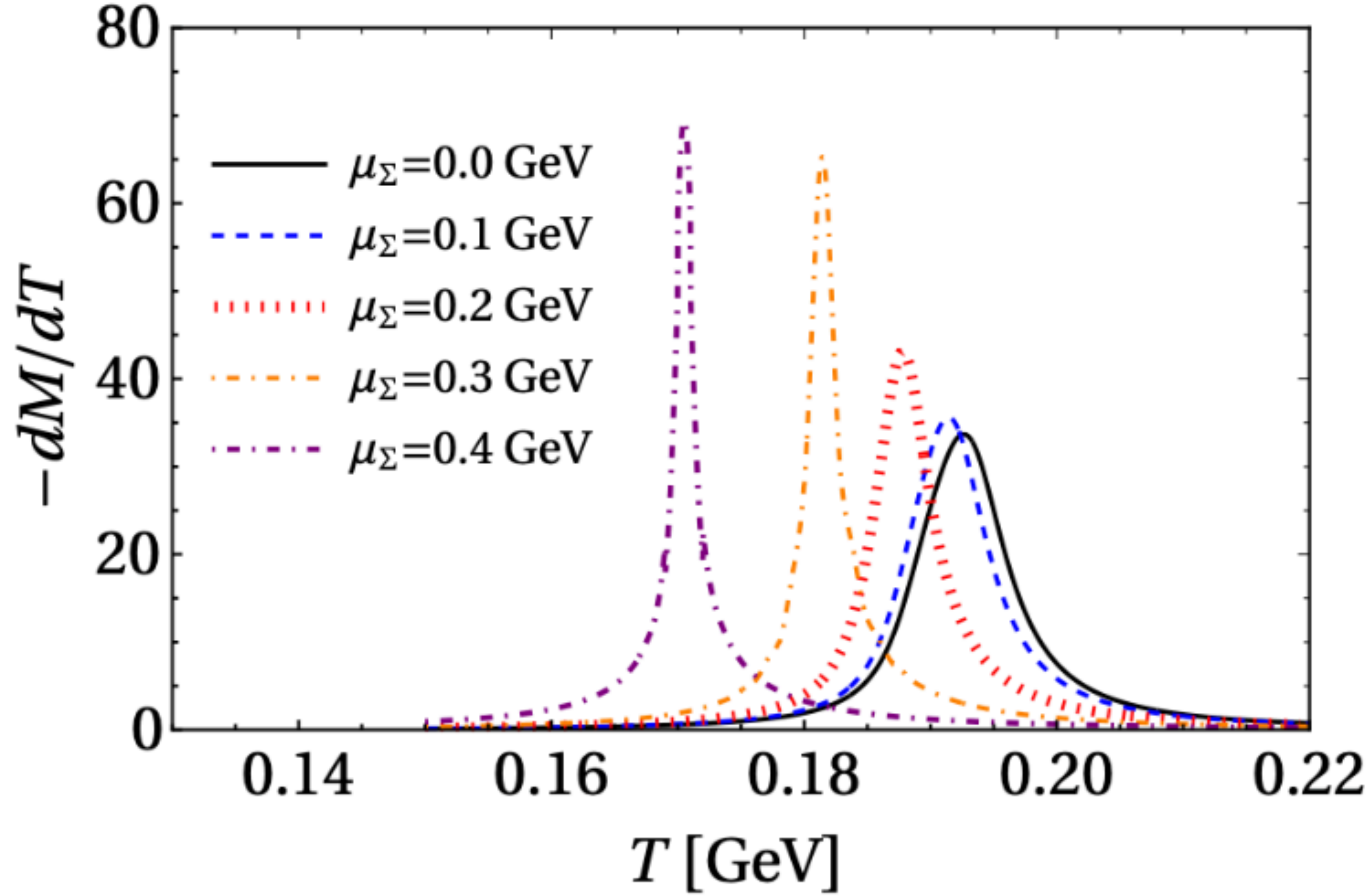

Numerical Results

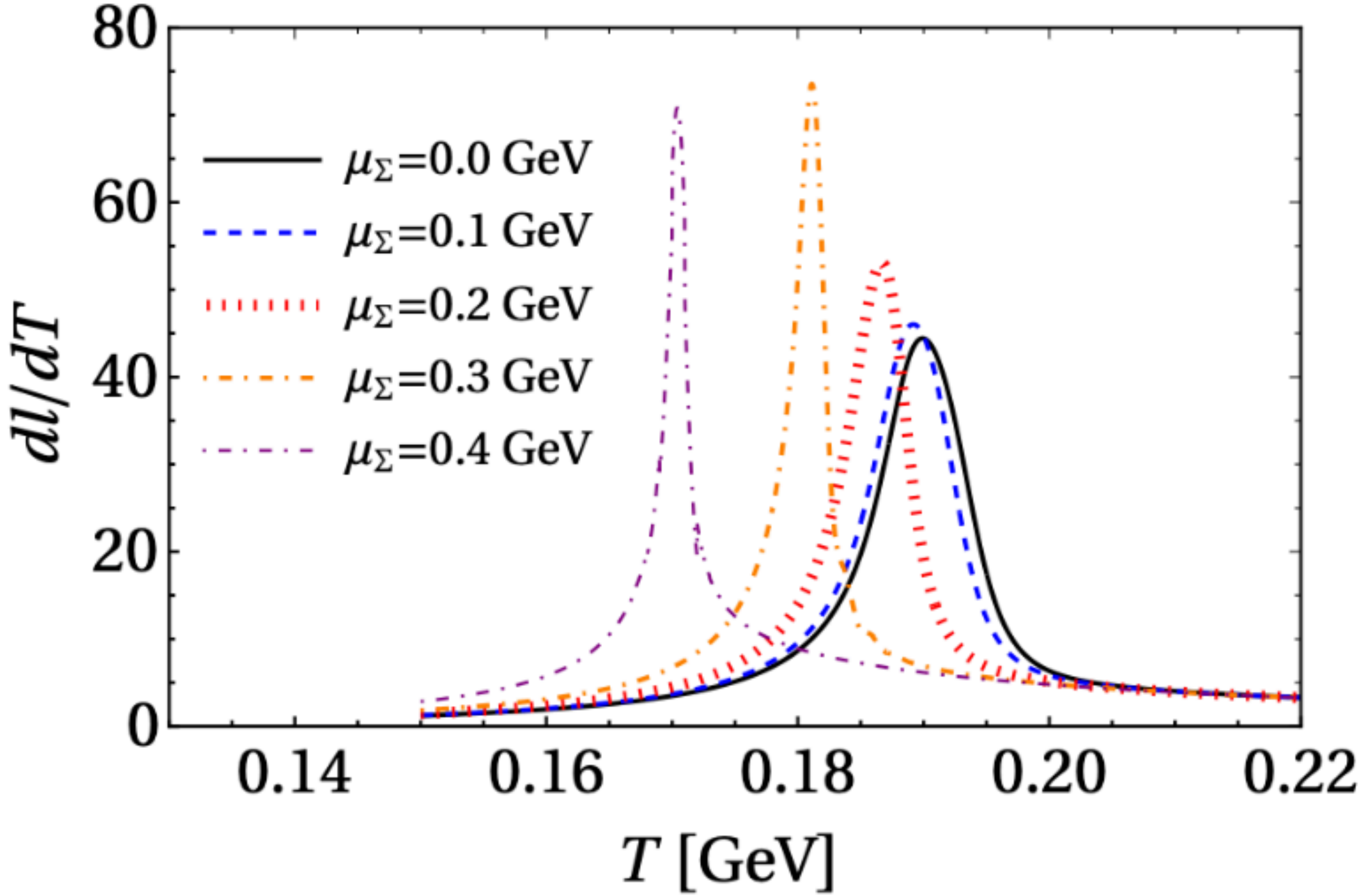

Numerical Results

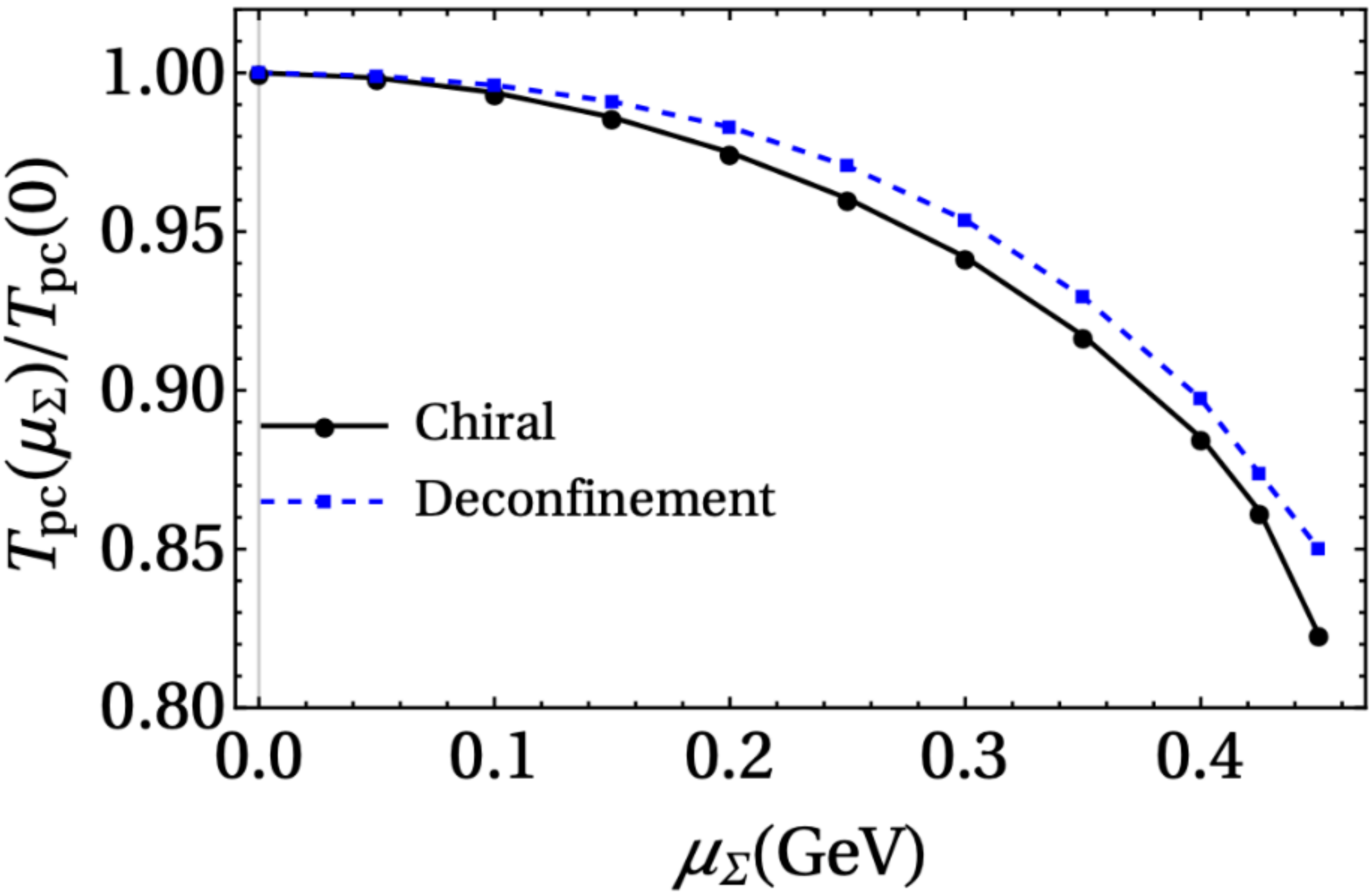

LQCD Results

$$T_c^\ell(\mu_\Sigma^{\rm I}) = T_c^\ell(0)\left[1 + \kappa_\Sigma^\ell \left(\frac{\mu_\Sigma^{\rm I}}{T}\right)^2\right]$$

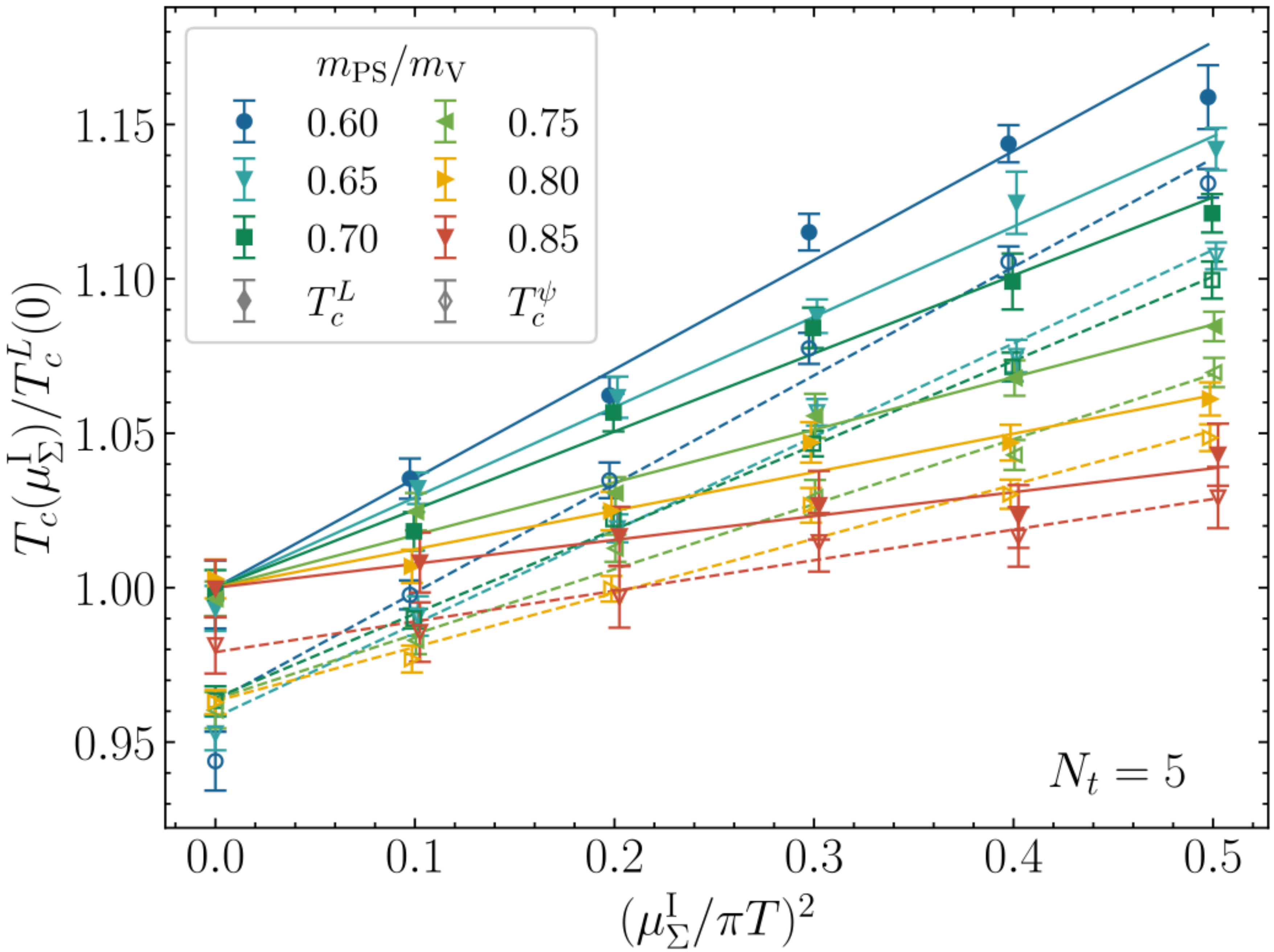

V. V. Braguta, M. N. Chernodub and A. A. Roenko, PRD **111**, 114508 (2025)

LQCD Results

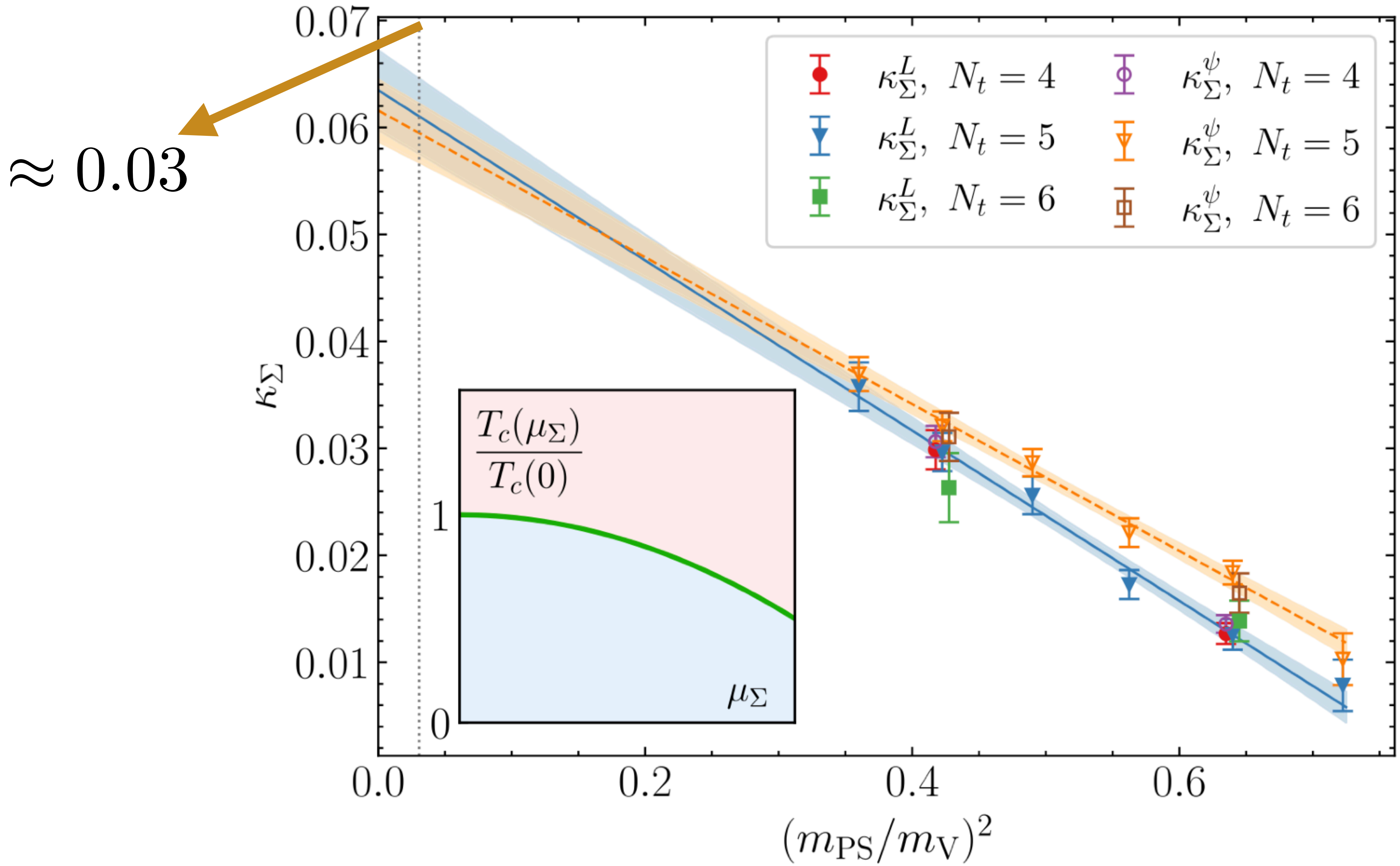

In EPNJL $\kappa^L \approx 0.028$ and $\kappa^\psi \approx 0.030$

V. V. Braguta, M. N. Chernodub and A. A. Roenko, PRD **111**, 114508 (2025)

Phase Diagram - Chiral transition

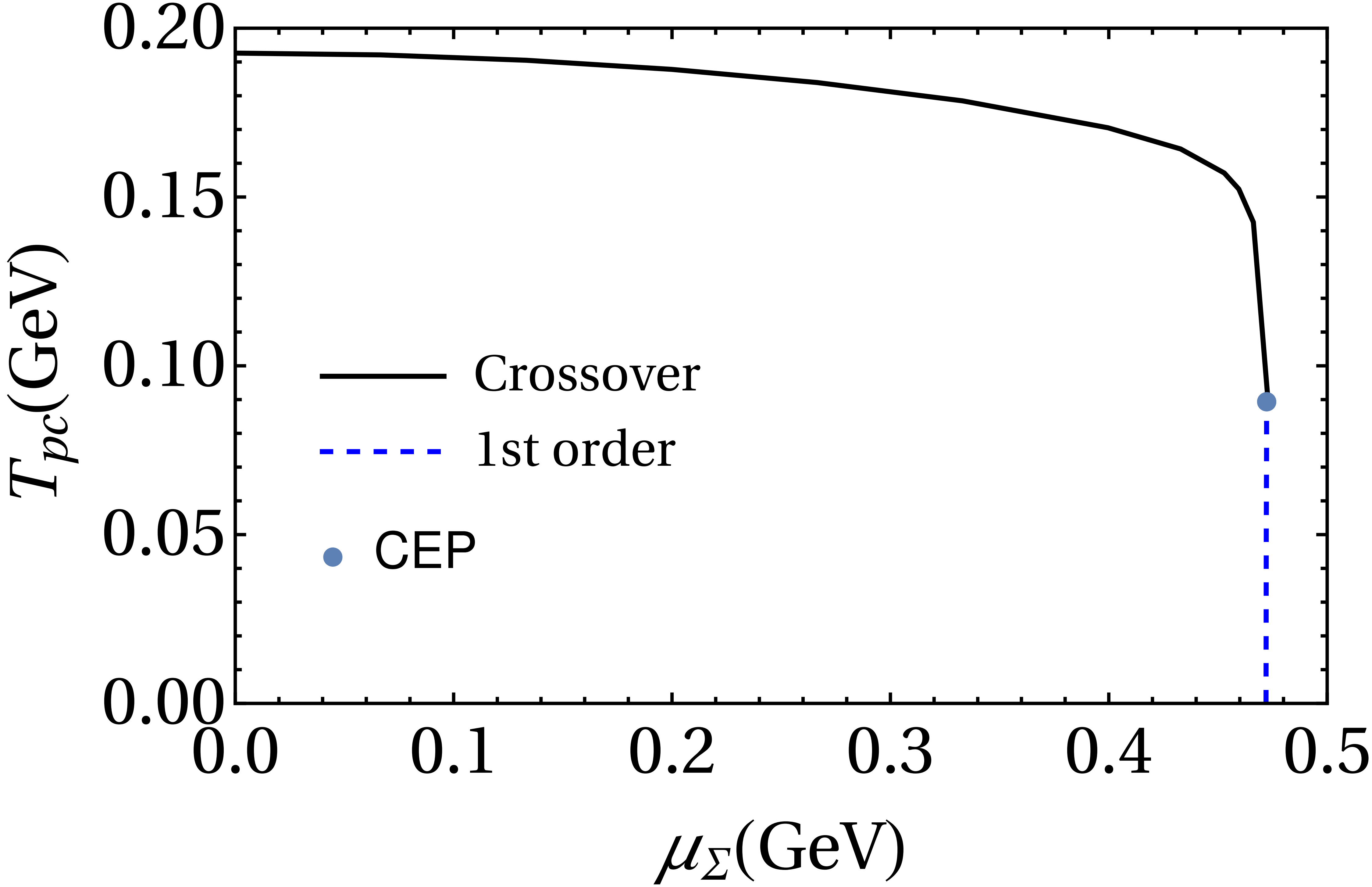

Working with spin potential:

- A cylindrical metric is not required
- Not constrained by slow-rotation considerations
- No worries about boundary conditions
- Causality violation is not a concern within this framework

Conclusions

- The finite spin density is introduced by the quark spin potential in the canonical formulation of the spin operator.
- LQCD and EPNJL model show that both chiral and deconfinement temperatures are decreasing functions of the spin potential.
- The phase diagram from EPNJL present a CEP at (0.472 GeV, 0.09 GeV)

Perspectives

- PQMM + T + μ_Σ

$$E_s^2 = p_\perp^2 + \left(\sqrt{p_3^2 + M^2} + s\frac{\mu_\Sigma}{2}\right)^2$$

Renormalization!

- Meson masses at finite spin potential
- Inclusion of baryonic density: $T \times \mu_B \times \mu_\Sigma$

μ_Σ Effects in QCD phase diagram

Conselho Nacional de Desenvolvimento Científico e Tecnológico

Thank you for your attention!

INSTITUTO NACIONAL DE CIÊNCIA E TECNOLOGIA
FÍSICA NUCLEAR E APLICAÇÕES